Magnetic Exchange through Oxalate Bridges: Synthesis and Characterization of (μ-Oxalato)dimetal(II) Complexes of Manganese, Iron, Cobalt, Nickel, Copper, and Zinc

Jørgen Glerup,*,[1a] Patricia A. Goodson,[1b] Derek J. Hodgson,*,[1c] and Kirsten Michelsen*,[1a]

Chemistry Laboratory I, H. C. Ørsted Institute, Universitetsparken 5,
DK-2100 Copenhagen Ø, Denmark, Department of Chemistry, University of Wyoming,
Laramie, Wyoming 82071, and Department of Chemistry, Mississippi State University,
Mississippi State, Mississippi 39762

Received March 22, 1995®

The syntheses and characterization of a series of binuclear μ-oxalato complexes of the general type $[(N)_4M(C_2O_4)M(N)_4]^{2+}$, where M is Mn^{II}, Fe^{II}, Co^{II}, Ni^{II}, Cu^{II}, and Zn^{II}, are described. The ligands $(N)_4$ represent the tetradentate ligands *N,N'*-bis(2-pyridylmethyl)-1,2-ethanediamine (bispicen, $C_{14}H_{18}N_4$), *N,N'*-bis(2-pyridylmethyl)-1,3-propanediamine (bispictn, $C_{15}H_{20}N_4$), and *N,N'*-bis(2-pyridylmethyl)-*N,N'*-dimethyl-1,2-ethanediamine (bispicMe₂en, $C_{16}H_{22}N_4$). The crystal structures of five representative complexes have been determined. The manganese complex $[(bispicen)Mn(C_2O_4)Mn(bispicen)](ClO_4)_2$ (**1a**) crystallizes in the noncentrosymmetric orthorhombic space group $Pna2_1$ with four binuclear formula units in a cell of dimensions $a = 21.771$ (4), $b = 23.650$ (5), and $c = 7.328$ (2) Å. The corresponding Fe(II), Cu(II), and Zn(II) complexes (**2a**, **5a**, and **6a**, respectively) are isomorphous with this manganese complex **1a**. The complex $[(bispicMe_2en)Mn(C_2O_4)Mn(bispicMe_2en)](ClO_4)_2$ (**1c**) crystallizes in the centrosymmetric monoclinic space group $P2_1/c$ with two binuclear formula units in a cell of dimensions $a = 9.218$ (2) Å, $b = 13.189$ (2) Å, $c = 17.213$ (3) Å, and $\beta = 92.780$ (10)°. The Co complex $[(bispicen)Co(C_2O_4)Co(bispicen)](ClO_4)_2\cdot H_2O$ (**3a**) crystallizes in the triclinic space group $P\bar{1}$ with one binuclear formula unit in a cell of dimensions $a = 8.832$ (2) Å, $b = 9.297$ (2) Å, $c = 13.045$ (3) Å, $\alpha = 108.01$ (3)°, $\beta = 98.48$ (3)°, and $\gamma = 93.31$ (3)°. The corresponding Ni(II) analogue, **4a**, is isomorphous with this cobalt complex. The copper(II) complex $[(bispicen)Cu(C_2O_4)Cu(bispicen)](ClO_4)_2$ (**5a**) is isomorphous with **1a**: $a = 21.531(4)$, $b = 23.708(5)$, and $c = 7.186(1)$ Å. The copper(II) complex $[(bispicMe_2en)Cu(C_2O_4)Cu(bispicMe_2en)](ClO_4)_2$ (**5c**) crystallizes in the centrosymmetric monoclinic space group $P2_1/n$ with two binuclear formula units in a cell of dimensions $a = 8.089$ (2) Å, $b = 22.001$ (4) Å, $c = 12.179$ (2) Å, and $\beta = 107.93$ (3)°. The corresponding Co(II), Ni(II), and Zn(II) complexes (**3c**, **4c**, and **6c**, respectively) are isomorphous with this copper complex. All five complexes contain six-coordinate metal centers bridged by planar bis-bidentate oxalate groups. The *J*-values for these oxalato bridged metal complexes are approximately 2, 6, 10, 33, and 2 cm^{-1} for Mn^{II}, Fe^{II}, Co^{II}, Ni^{II}, and Cu^{II}, respectively. This is explained as a result of the magnetic interaction between the x^2-y^2 orbitals on the two metal atoms, and in spite of the difference between the *J*-values for these complexes it is shown that the interaction matrix element between these orbitals have approximately the same value for the Mn^{II}, Fe^{II}, Co^{II}, and Ni^{II} complexes. The small *J*-values for the Cu^{II} complexes are caused by the fact that in these cases the x^2-y^2 orbitals are not the magnetic orbitals.

Introduction

The study of magnetic interactions in di- and polynuclear metal complexes as a function of geometry and electron configuration of the individual metal atoms is still a main issue in inorganic chemistry. The bridging ligands can be divided into two groups, one where one atom forms the bridge and one where several atoms form the bridge, *i.e.*, in the first case the two metals have the same ligator atom, and in the second case the two metals have different ligator atoms. Typical examples of the first group are bridges like μ-oxo and μ-hydroxo, while the second group is represented by bridges like μ-acetato, μ-oxalato, and μ-cyano. The latter group gives rise to several problems in the discussion of the magnetic interactions.

The magnetic interactions of dinuclear oxalato bridged complexes have been thoroughly discussed by Hoffmann[2] on the basis of molecular orbital theory. In a series of papers Kahn and colleagues[3] has described a theory to predict the magnetic interactions in oxalate bridge Cu^{II} complexes. The theories presented by these authors have been used to rationalize the magnetic interactions observed for oxalato bridged Cu^{II},[4–6] Ni^{II},[4a,7] and Ti^{III} [8] complexes.

The simple binuclear geometry involving symmetric, in-plane bridging with a single oxalate ion binding through two oxygen atoms to each of two metal centers has been observed in the chemistry of nickel(II)[4a,7] and (less frequently) zinc(II),[4a] but while mononuclear[9] and chain[10] structures have been observed, it is unknown in the structural chemistry of chromium,

---

® Abstract published in *Advance ACS Abstracts,* November 1, 1995.

[1] (a) University of Copenhagen. (b) University of Wyoming. (c) Mississippi State University.

[2] Hay, G. R.; Thibeault, J. C.; Hoffmann, R. *J. Am. Chem. Soc.* **1975**, *97*, 4884–4899.

[3] (a) Julve, M.; Verdaguer, M.; Kahn, O.; Gleizes, A.; Philoche-Levisalles, M. *Inorg. Chem.* **1983**, *22*, 368–370. (b) Julve, M.; Verdaguer, M.; Gleizes, A.; Philoche-Levisalles, M.; Kahn, O. *Inorg. Chem.* **1984**, *23*, 3808–3818.

[4] (a) Curtis, N. F.; McCormick, I. R. N.; Waters, T. N. *J. Chem. Soc., Dalton Trans.* **1973**, 1537–1548. (b) Felthouse, T. R.; Laskowski, E. J.; Hendrickson, D. N. *Inorg. Chem.* **1977**, *16*, 1077–1089. (c) Kansikas, J.; Pajunen, A. *Acta Crystallogr., Sect. B* **1980**, *36*, 2423–2425. (d) Sletten, J. *Acta Chem. Scand. Ser. A* **1983**, *A37*, 569–578.

[5] (a) Castro, I.; Faus, J.; Julve, M.; Mollar, M.; Monge, A.; Gutierrez-Puebla, E. *Inorg. Chim. Acta* **1989**, *161*, 97–104. (b) Castro, I.; Faus, J.; Julve, M.; Munoz, M. C.; Diaz, W.; Solans, X. *Inorg. Chim. Acta* **1991**, *179*, 59–66. (c) Castro, I.; Faus, J.; Julve, M.; Gleizes, A. *J. Chem. Soc., Dalton Trans.* **1991**, 1937–1944. (d) George, C.; Purdy, A. *Acta Crystallogr., Sect. C* **1992**, *48*, 155–157.

0020-1669/95/1334-6255$09.00/0

Table 1. Analytical Data for the Complexes $[(N)_4M(C_2O_4)M(N)_4](ClO_4)_2{\cdot}xH_2O$

M	$(N)_4$	x	found (calcd)			
			C	N	H	Cl
Mn	bispicen	0	40.72 (40.88)	12.79 (12.71)	4.02 (4.12)	8.15 (8.04)
Fe	bispicen	0	40.41 (40.79)	12.77 (12.69)	4.10 (4.11)	7.95 (8.03)
Co	bispicen	0	37.89 (38.19)	11.96 (11.88)	4.46 (4.49)	7.56 (7.52)
Ni	bispicen	3	37.84 (38.20)	12.01 (11.88)	4.18 (4.49)	7.26 (7.52)
Zn	bispicen	0	39.72 (39.93)	12.47 (12.42)	4.09 (4.02)	7.83 (7.86)
Cu	bispicen	0	39.82 (40.10)	12.46 (12.47)	3.98 (4.04)	7.97 (7.89)
Mn	bispictn	$^1/_2$	41.75 (41.85)	12.17 (12.20)	4.33 (4.50)	7.65 (7.72)
Fe	bispictn	$^1/_2$	41.75 (41.76)	12.10 (12.18)	4.46 (4.49)	8.02 (7.70)
Co	bispictn	1	40.94 (41.09)	11.98 (11.98)	4.33 (4.53)	7.76 (7.58)
Ni	bispictn	1	41.05 (41.10)	12.14 (11.98)	4.36 (4.53)	8.13 (7.58)
Zn	bispictn	$^1/_2$	41.00 (40.92)	12.05 (11.93)	4.19 (4.40)	7.54 (7.55)
Mn	bispicMe$_2$en	0	43.55 (43.56)	11.68 (11.95)	4.69 (4.73)	7.36 (7.57)
Fe	bispicMe$_2$en	1	42.90 (42.65)	11.64 (11.70)	4.64 (4.84)	7.49 (7.41)
Co	bispicMe$_2$en	1	42.55 (42.38)	11.59 (11.63)	4.62 (4.81)	7.42 (7.36)
Ni	bispicMe$_2$en	1	42.45 (42.40)	11.78 (11.63)	4.56 (4.81)	7.36 (7.36)
Zn	bispicMe$_2$en	0	42.82 (42.60)	11.67 (11.69)	4.49 (4.63)	6.47 (7.40)
Cu	bispicMe$_2$en	0	42.46 (42.77)	11.69 (11.74)	4.76 (4.65)	7.68 (7.43)

manganese, iron, and cobalt. With the purpose of examining the magnetic interactions as functions of the electronic configuration of the individual metal atoms, we have succeeded in synthesizing a related series of complexes of these first-row metals of the general formulation $[(N)_4M(ox)M(N)_4]^{2+}$, where $(N)_4$ represents a tetradentate nitrogen donor, ox is the oxalato dianion, and M is Mn, Fe, Co, Ni, Cu, or Zn. We report here the syntheses and structural and magnetic characterization of these complexes, where the tetradentate ligands used are *N,N'*-bis(2-pyridylmethyl)-1,2-ethanediamine (bispicen, $C_{14}H_{18}N_4$), *N,N'*-bis(2-pyridylmethyl)-1,3-propanediamine (bispictn, $C_{15}H_{20}N_4$), and *N,N'*-bis(2-pyridylmethyl)-*N,N'*-dimethyl-1,2-ethanediamine, (bispicMe$_2$en, $C_{16}H_{22}N_4$).

Experimental Section

Physical Measurements. The magnetic susceptibilities of powdered samples were measured by the Faraday method in the temperature range 2−300 K at a field strength of 1.3 T. The susceptibility data were corrected for diamagnetism by Pascal's constants. The magnetic field was calibrated with $Hg[Co(NCS)_4]$.[11] A more detailed description of the equipment is published elsewhere.[12] EPR spectra were recorded on a Bruker ESP-300 spectrometer equipped with an Oxford ESR-9 gas-flow cryostat. The metal analyses were performed on a Perkin-Elmer 403 atomic absorption spectrometer. ^{13}C NMR spectra were recorded at room temperature on a Bruker MSL 300 spectrometer; samples were examined as solids. X-ray powder diagrams were obtained on a Guinier camera using Cu Kα radiation. The microanalytical laboratory of the H. C. Ørsted Institute carried out analyses for carbon, nitrogen, hydrogen, halogen, and sulfur by standard methods.

Synthetic Methods. *Caution! The complexes described here were isolated as perchlorate salts and should be handled as potentially explosive compounds. Mother liquors containing even small amounts of perchloric acid should never be mixed with washing liquors containing ethanol.*

Ligands. The preparations of the tetrahydrochlorides of bispicen, bispictn, and bispicMe$_2$en have been described before.[13−15]

(μ-Oxalato)bis(tetramine)dimanganese(II) Perchlorate, $[(N)_4Mn^{II}(C_2O_4)Mn^{II}(N)_4](ClO_4)_2{\cdot}xH_2O$ (1a−c; $(N)_4$ = bispicen, bispictn, bispicMe$_2$en). In a small conical flask bispicen·4HCl·2H$_2$O (0.127 g, 0.30 mmol) was dissolved in water (3 mL). The solution was neutralized with a solution of sodium carbonate (1 M), and nitrogen was bubbled through for 5 min. A solution of manganese(II) chloride tetrahydrate (0.059 g, 0.30 mmol) in water (1 mL) was added, followed by a solution of ammonium oxalate (0.5 mL, 0.3 M). The nitrogen flow was continued for 5 min. A solution of sodium perchlorate (1 mL, 1 M) deaerated with nitrogen was added, and the flask was stoppered and set aside for 24 h. The white crystals that had separated were filtered and washed with a solution of sodium perchlorate (1 M) and with ethanol (96%). Yield of $[(bispicen)Mn(C_2O_4)Mn(bispicen)](ClO_4)_2$ (**1a**): 0.074 g (52%). Corresponding complexes with bispictn and bispicMe$_2$en could be synthesized by the same method but from bispictn·4 HCl·2 H$_2$O (0.133 g, 0.30 mmol) and bispicMe$_2$en·4HCl (0.125 g, 0.30 mmol) respectively. Yield of $[(bispictn)Mn(C_2O_4)Mn(bispictn)](ClO_4)_2{\cdot}0.5H_2O$ (**1b**): 0.108 g (78%). Yield of $[(bispicMe_2en)Mn(C_2O_4)Mn(bispicMe_2en)](ClO_4)_2$ (**1c**): 0.082 g (58%). Analytical data are summarized in Table 1.

(μ-Oxalato)bis(tetramine)diiron(II) Perchlorate, $[(N)_4Fe^{II}(C_2O_4)Fe^{II}(N)_4](ClO_4)_2{\cdot}xH_2O$ (2a−c); $(N)_4$ = bispicen, bispictn, bispicMe$_2$en). The complexes were synthesized exactly as the corresponding manganese(II) complexes but from iron(II) sulfate heptahydrate (0.083 g, 0.30 mmol). Yield of yellow-green $[(bispicen)Fe(C_2O_4)Fe(bispicen)](ClO_4)_2$ (**2a**): 0.040 g (30%). Yield of yellow-green $[(bispictn)Fe(C_2O_4)F(ebispictn)](ClO_4)_2{\cdot}0.5H_2O$ (**2b**): 0.061 g (44%). Yield of yellow $[(bispicMe_2en)Fe(C_2O_4)Fe(bispicMe_2en)](ClO_4)_2{\cdot}H_2O$ (**2c**): 0.065 (45%). Analytical data are summarized in Table 1.

(μ-Oxalato)bis(tetramine)dicobalt(II) Perchlorate, $[(N)_4Co^{II}(C_2O_4)Co^{II}(N)_4](ClO_4)_2{\cdot}xH_2O$ (3a−c); $(N)_4$ = bispicen, bispictn, bispicMe$_2$en). The compounds were synthesized exactly as the

---

(6) (a) Julve, M.; Faus, J.; Verdaguer, M.; Gleizes, A. *J. Am. Chem. Soc.* **1984**, *106*, 8306−8308. (b) Bencini, A.; Fabretti, A. C.; Zanchini, C.; Zannini, P. *Inorg. Chem.* **1987**, *26*, 1445−1449. (c) Soto, L.; Garcia, J.; Escriva, E.; Legros, J.-P.; Tuchagues, J.-P.; Dahan, F.; Fuertes, A. *Inorg. Chem.* **1989**, *28*, 3378−3386. (d) Soto-Tuero, L.; Garcia-Lozano, J.; Escriva-Monto, E. E.; Beneto-Borja, M.; Dahan, F.; Tuchagues, J.-P.; Legros, J.-P. *J. Chem. Soc., Dalton Trans.* **1991**, 2619−2624.

(7) (a) Duggen, D. M.; Barefield, E. K.; Hendrickson, D. N. *Inorg. Chem.* **1972**, *12*, 985−991. (b) Davis, A. R.; Einstein, F. W. B.; Willis, A. C. *Acta Crystallogr., Sect. B* **1982**, *38*, 443−448. (d) Alcock, N. W.; Moore, P.; Omar, H. A. A. *Acta Crystallogr., Sect. C* **1987**, *43*, 2074−2076. (e) Klein, H.-F.; Wiemer, T.; Menu, M.-J.; Dartiguenave, M.; Dartiguenave, Y. *Inorg. Chim. Acta* **1988**, *154*, 21−29. (f) Battaglia, L. P.; Bianchi, A.; Corradi, A. B.; Garcia-Espana, E.; Micheloni, M.; Julve, M. *Inorg. Chem.* **1988**, *27*, 4174−4179. (g) Bencini, A.; Bianchi, A.; Paoli, P.; Garcia-Espana, E.; Julve, M.; Marcelino, V. *J. Chem. Soc., Dalton Trans.* **1990**, 2213−2217. (h) Bencini, A.; Bianchi, A.; Garcia-Espana, E.; Jeannin, Y.; Julve, M.; Marcelino, V.; Philoche-levisalles, M. *Inorg. Chem.* **1990**, *29*, 963−970.

(8) Harris, A. H.; Kanis, D. R.; Dahl, L. F. *J. Am. Chem. Soc.* **1991**, *113*, 8602−8611.

(9) See, for example: Van Niekerk, J. N.; Schoening, F. R. L. *Acta Crystallogr.* **1952**, *5*, 499−505.

(10) See, for example: Deguenon, D.; Bernardinelli, G.; Tuchagues, J.-P.; Castan, P. *Inorg. Chem.* **1990**, *29*, 3031−3037.

(11) Figgis, B. N.; Nyholm, R. S. *J. Chem. Soc.* **1958**, 4190−4191.

(12) Pedersen, E. *Acta Chem. Scand.* **1972**, *26*, 333−342.

(13) Michelsen, K. *Acta Chem. Scand.* **1977**, *A31*, 429−436.

(14) Fischer, H. R.; Hodgson, D. J.; Michelsen, K.; Pedersen, E. *Inorg. Chim. Acta* **1984**, *88*, 143−150.

(15) Glerup, J.; Goodson, P. A.; Hazell, A.; Hodgson, D. J.; McKenzie, C. J.; Michelsen, K.; Rychlewska, U.; Toftlund, H. *Inorg. Chem.* **1994**, *33*, 3023−3025.

Table 2. Crystallographic Data for the Complexes **1a, 1c, 3a, 5a,** and **5c**

	1a	**1c**	**3a**	**5a**	**5c**
formula	$C_{30}H_{36}Cl_2Mn_2N_8O_{12}$	$C_{34}H_{44}Cl_2Mn_2N_8O_{12}$	$C_{30}H_{38}Cl_2Co_2N_8O_{13}$	$C_{30}H_{36}Cl_2Cu_2N_8O_{12}$	$C_{34}H_{44}Cl_2Cu_2N_8O_{12}$
fw	881.4	937.6	907.4	898.6	954.8
a, Å	21.771 (4)	9.218 (2)	8.832 (2)	21.531 (4)	8.089 (2)
b, Å	23.650 (5)	13.189 (2)	9.297 (2)	23.708 (5)	22.001 (4)
c, Å	7.328 (2)	17.213 (3)	13.045 (3)	7.186 (2)	12.179 (2)
α,deg	90	90	108.01 (3)	90	90
β,deg	90	92.78 (1)	98.48 (3)	90	107.93 (3)
γ,deg	90	90	93.31 (3)	90	90
V, Å^3	3773 (2)	2090.2 (7)	1001.4 (4)	3668 (2)	2062.0 (7)
Z	4	2	1	4	2
space group	$Pna2_1$	$P2_1/c$	$P\bar{1}$	$Pna2_1$	$P2_1/n$
T, °C	23	22	23	23	22
λ, Å	0.710 73	0.710 73	0.710 73	0.710 73	0.710 73
ρ_{calc}, g/cm^3	1.552	1.490	1.504	1.627	1.538
μ, mm^{-1}	0.881	0.774	1.031	1.377	1.230
R^a	0.0761	0.0429	0.0534	0.0799	0.0440
$R_w{}^b$	0.0669	0.0532	0.0647	0.0807	0.0499

[a] $R = \Sigma||F_o|-|F_c||/\Sigma|F_o|$. [b] $R_w = [\Sigma w(|F_o| - |F_c|)^2/\Sigma w|F_o|^2]^{1/2}$.

corresponding complexes with manganese(II) but from cobalt(II) chloride hexahydrate (0.071 g, 0.30 mmol). Yield of crystals of yellow-pink [(bispicen)Co(C_2O_2)Co(bispicen)](ClO_4)$_2$·$3H_2O$ (**3a**): 0.074 g (52%). Yield of [(bispictn)Co(C_2O_2)Co(bispictn)](ClO_4)$_2$·H_2O (**3b**): 0.068 g (48%). Yield of [(bispicMe$_2$en)Co(C_2O_4)Co(bispicMe$_2$en)](ClO_4)$_2$·H_2O (**3c**): 0.109 g (75%). Analytical data are summarized in Table 1.

(μ-Oxalato)bis(tetramine)dinickel(II) Perchlorate, [(N)$_4$Ni(C_2O_4)$_2$Ni(N)$_4$](ClO_4)$_2$·$x$$H_2O$ (4a–c); (N)$_4$ = bispicen, bispictn, bispicMe$_2$en). In a small beaker bispicen·4HCl·$2H_2O$ (0.127 g, 0.30 mmol) was dissolved in water (3 mL). As described above, the solution was neutralized with sodium carbonate (1 M), and nickel chloride hexahydrate (0.071 g, 0.30 mmol) dissolved in water (1 mL) was added followed by solutions of ammonium oxalate (0.5 mL, 0.3 M) and sodium perchlorate (1M). After 24 h violet crystals of [(bispicen)Ni(C_2O_4)Ni(bispicen)](ClO_4)$_2$·$3H_2O$ (**4a**; 0.063 g (45%)) were filtered and washed as described above. The violet complexes [(bispictn)Ni(C_2O_4)Ni(bispictn)](ClO_4)$_2$·H_2O (**4b**; 0.061 g (43%)) and [(bispicMe$_2$en)Ni(C_2O_4)Ni(bispicMe$_2$en)](ClO_4)$_2$·H_2O (**4c**; 0.115 g (80%)) were synthesized similarly from the appropriate ligand hydrochlorides. Analytical data are summarized in Table 1.

(μ-Oxalato)bis(tetramine)dicopper(II) Perchlorate, [(N)$_4$Ni(C_2O_4)$_2$Ni(N)$_4$](ClO_4)$_2$·$x$$H_2O$ (5a,c); (N)$_4$ = bispicen, bispicMe$_2$en). [(bispicMe$_2$en)Cu(C_2O_4)Cu(bispicMe$_2$en)](ClO_4)$_2$ (**5c**) was synthesized exactly as the corresponding nickel complex but from copper chloride dihydrate (0.075 g, 0.30 mmol). Yield of sky-blue elongated crystals : 0.115 g (80%). [(bispicen)Cu(C_2O_4)Cu(bispicen)](ClO_4)$_2$·$x$$H_2O$ (**5a**) was synthesized as the corresponding nickel complex but from copper sulfate pentahydrate (0.075 g, 0.30 mmol). Yield of sky-blue elongated crystals: 0.071 g (53%). If copper chloride dihydrate was used as a starting material in this case, violet crystals with an analysis fitting the formulation of [Cu(bispicen)](ClO_4)$_2$ or marine-blue crystals with an analysis fitting that of [Cu(bispicen)Cl](ClO_4) resulted instead. These compounds could be converted to the oxalato bridged complexes if they were boiled with a solution of ammonium oxalate. It was, however, never possible to isolate an oxalato bridged copper(II) complex with bispictn (*i.e.*, a putative **5b**). The result was always violet crystals with an analysis fitting [Cu(bispictn)](ClO_4)$_2$·$0.5H_2O$. Analytical data for the oxalato complexes are summarized in Table 1.

(μ-Oxalato)bis(tetramine)dizinc(II) Perchlorate, [(N)$_4$Zn(C_2O_4)$_2$Zn(N)$_4$](ClO_4)$_2$·$x$$H_2O$ (6a–c); (N)$_4$ = bispicen, bispictn, bispicMe$_2$en). These complexes were synthesized as the corresponding complexes with nickel but from zinc nitrate hexahydrate (0.089 g, 0.30 mmol). Yields of white crystals of [(bispicen)Zn(C_2O_4)Zn(bispicen)](ClO_4)$_2$ (**6a**): 0.103 g (76%). Yield of [(bispictn)Zn(C_2O_4)Zn(bispictn)](ClO_4)$_2$·$0.5H_2O$ (**6b**): 0.095 g (67%). Yield of [(bispicMe$_2$en)Zn(C_2O_4)Zn(bispicMe$_2$en)](ClO_4)$_2$ (**6c**): 0.127 g (88%). Analytical data are summarized in Table 1.

Table 3. Selected Atomic Coordinates (×10^4) and Equivalent Isotropic Displacement Coefficients (Å^2 × 10^3) for Complex **1a**

	x	y	z	U(eq)^a
Mn(1)	1223(1)	6308(1)	1375	42(1)
Mn(2)	2970(2)	5258(1)	5904(7)	41(1)
N(1)	499(7)	5653(7)	1197(30)	42(5)
N(2)	349(8)	6795(7)	713(29)	54(6)
N(3)	1462(8)	6607(8)	−1497(28)	48(6)
N(4)	1869(9)	7049(8)	1684(30)	57(6)
N(5)	3811(8)	4843(8)	4781(26)	48(5)
N(6)	2775(9)	4317(8)	6186(39)	78(6)
N(8)	3494(8)	6023(8)	6877(25)	50(6)
N(7)	3018(9)	5178(8)	8962(25)	52(6)
O(1)	1381(7)	6111(6)	4236(21)	45(4)
O(2)	2025(6)	5754(5)	1262(23)	45(4)
O(3)	2750(7)	5434(6)	3102(23)	62(5)
O(4)	2053(6)	5643(5)	6034(24)	45(4)

[a] Equivalent isotropic U is defined as one third of the trace of the orthogonalized $\mathbf{U}_{ij}$ tensor.

X-ray Structure Determination. The structures of complexes **1a**, **1c**, **3a**, **5a**, and **5c** were determined at room temperature (295 K) on a Nicolet R3m/V diffractometer equipped with a molybdenum tube [λ(Kα_1) = 0.709 26 Å; λ(Kα_2) = 0.713 54 Å] and a graphite monochromator. Crystal data and experimental parameters are presented in Table 2. The data were corrected for Lorentz–polarization effects and absorption. The structures were solved by direct methods and refined by least-squares techniques; the programs used were from the SHELX-TL IRIS system.[16]

(μ-Oxalato)bis(N,N'-bis(2-pyridylmethyl)-1,2-ethanediamine)dimanganese(II) Perchlorate, [(bispicen)Mn(C_2O_4)Mn(bispicen)](ClO_4)$_2$ (1a). The complex crystallizes in the noncentrosymmetric orthorhombic space group $Pna2_1$ with four binuclear formula units in the unit cell. X-ray powder patterns indicate that the corresponding Fe(II), Cu(II), and Zn(II) complexes [**2a**, **5a**, and **6a**, respectively] are isomorphous, and presumably isostructural, with this manganese complex **1a**; the Co(II) and Ni(II) analogues, **3a** and **4a**, are not isomorphous with these complexes (*vide infra*). Data were collected in the range $4 < 2\theta < 45°$, the data gathered having $0 \le h \le +23$, $0 \le k \le +25$, $-7 \le l \le 0$. All hydrogen atoms were placed in fixed calculated positions (C–H = 0.96 Å; N–H = 0.90 Å). Because of the paucity of data, only the Mn and the perchlorate chlorine and oxygen atoms could be refined anisotropically, the other non-hydrogen atoms being refined isotropically. The final values of the conventional R factors were $R = 0.0761$, $R_w = 0.0669$, based on 1367 independent reflections with $I > 2\sigma(I)$. Positional parameters are listed in Table 3.

(μ-Oxalato)bis(N,N'-bis(2-pyridylmethyl)-N,N'-bis(methyl)-1,2-ethanediamine)dimanganese(II) Perchlorate, [(bispicMe$_2$en)Mn(C_2O_4)Mn(bispicMe$_2$en)](ClO_4)$_2$ (1c). The complex crystallizes in the centrosymmetric monoclinic space group $P2_1/c$ with two binuclear formula units in the cell. Data were collected in the range $4 < 2\theta <$

---

(16) Sheldrick, G. M. *SHELXTL-PLUS Crystallographic System*, Version 2; Nicolet XRD Corp.: Madison, WI, 1987.

Table 4. Selected Atomic Coordinates ($\times 10^4$) and Equivalent Isotropic Displacement Coefficients (Å^2 $\times$ 10^3) for Complex **1c**

	x	*y*	*z*	*U*(eq)[a]
Mn(1)	8764(1)	1491(1)	923(1)	41(1)
O(1)	9058(3)	1103(2)	−283(2)	45(1)
O(2)	10041(3)	120(2)	1010(2)	49(1)
N(1A)	10583(4)	2627(3)	849(2)	51(1)
N(2A)	9134(4)	2135(3)	2154(2)	47(1)
N(1B)	6702(4)	597(3)	1026(2)	44(1)
N(2B)	6935(4)	2662(2)	923(2)	43(1)

[a] See footnote *a* of Table 3.

Table 5. Selected Atomic Coordinates ($\times 10^4$) and Equivalent Isotropic Displacement Coefficients (Å^2 $\times$ 10^3) for Complex **3a**

	x	*y*	*z*	*U*(eq)[a]
Co(1)	1735(1)	1297(1)	2020(1)	46(1)
N(1)	186(5)	443(5)	2857(4)	60(2)
N(2)	1729(6)	3211(5)	3452(3)	65(2)
N(3)	3944(5)	1162(5)	2899(3)	59(2)
N(4)	3320(5)	2153(5)	1189(3)	53(2)
O(1)	−137(3)	1718(3)	1007(3)	48(1)
O(2)	1433(3)	−730(3)	697(3)	48(1)

[a] See footnote *a* of Table 3.

50°, the data gathered having $-10 \le h \le 0$, $0 \le k \le +15$, $-20 \le l \le +20$. Hydrogen atoms were placed in fixed calculated positions (C−H = 0.96 Å); non-hydrogen atoms were refined anisotropically. The final values of the conventional *R* factors were $R = 0.0429$, $R_w = 0.0532$ based on 2341 independent reflections with $I > 3\sigma(I)$. Positional parameters are listed in Table 4.

(μ-Oxalato)bis(*N*,*N'*-bis(2-pyridylmethyl)-1,2-ethanediamine)dicobalt(II) Perchlorate, [(bispicen)Co(C_2O_4)Co(bispicen)](ClO_4)$_2$·H_2O (3a). The complex crystallizes in the triclinic space group $P\bar{1}$ with one binuclear formula unit in the cell. X-ray powder patterns indicate that the corresponding Ni(II) analogue, **4a**, is isomorphous with this cobalt complex, so that the six bispicen complexes fall into two isomorphous series (*vide supra*). Data were collected in the range $4 < 2\theta < 55°$, the data gathered having $0 \le h \le +12$, $-13 \le k \le +13$, $-17 \le l \le +17$. Hydrogen atoms associated with the solvent water molecule were not located, while hydrogen atoms bound to carbon and nitrogen atoms were placed in fixed calculated positions (C−H = 0.96 Å, N−H = 0.90 Å); all non-hydrogen atoms were refined anisotropically. The final values of the conventional *R* factors were $R = 0.0534$, $R_w = 0.0647$ based on 2475 independent reflections with $I > 3\sigma(I)$. Positional parameters are listed in Table 5.

(μ-Oxalato)bis(*N*,*N'*-bis(2-pyridylmethyl)-1,2-ethanediamine)dicopper(II) Perchlorate, [(bispicen)Cu(C_2O_4)Cu(bispicen)](ClO_4)$_2$ (5a). The complex is isomorphous with **1a**. Data were collected in the range $4 < 2\theta < 45°$, the data gathered having $-23 \le h \le 0$, $-25 \le k \le 0$, $0 \le l \le +7$. Hydrogen atoms were placed in fixed calculated positions (C−H = 0.96 Å; N−H = 0.90 Å); all non-hydrogen atoms were refined anisotropically. The final values of the conventional *R* factors were $R = 0.0799$ and $R_w = 0.0808$ based on 1575 independent reflections with $I > 2\sigma(I)$. Positional parameters are listed in Table 6.

Table 6. Selected Atomic Coordinates ($\times 10^4$) and Equivalent Isotropic Displacement Coefficients (Å^2 $\times$ 10^3) for Complex **5a**

	x	*y*	*z*	*U*(eq)[a]
Cu(1)	3798(1)	6308(1)	1917	37(1)
Cu(2)	2050(1)	5255(1)	6542(6)	38(1)
O(1)	3707(8)	6084(6)	4831(24)	46(5)
O(2)	2983(7)	5734(5)	1773(30)	46(4)
O(3)	3082(6)	5593(5)	6723(29)	44(4)
O(4)	2275(7)	5424(6)	3899(24)	41(4)
N(1)	4444(7)	5694(6)	1735(33)	37(4)
N(2)	4619(9)	6815(8)	1490(37)	61(6)
N(3)	3598(9)	6527(8)	−1003(29)	46(6)
N(4)	3201(9)	6959(7)	2207(28)	41(5)
N(5)	1632(9)	5970(8)	7212(30)	52(6)
N(6)	2045(10)	5168(8)	9234(28)	44(6)
N(7)	2337(8)	4431(7)	6450(29)	38(5)
N(8)	1203(10)	4860(8)	5403(30)	50(6)

[a] See footnote *a* of Table 3.

Table 7. Selected Atomic Coordinates ($\times 10^4$) and Equivalent Isotropic Displacement Coefficients (Å^2 $\times$ 10^3) for Complex **5c**

	x	*y*	*z*	*U*(eq)[a]
Cu(1)	1320(1)	890(1)	3925(1)	34(1)
O(1)	1595(6)	−25(2)	4298(4)	45(2)
O(2)	−579(5)	764(2)	4849(4)	45(2)
N(1)	3260(7)	1076(2)	5414(5)	40(2)
N(2)	3537(7)	1016(3)	3264(4)	44(2)
N(3)	698(7)	1796(3)	3331(5)	45(2)
N(4)	−592(7)	733(3)	2402(5)	45(2)

[a] See footnote *a* of Table 3.

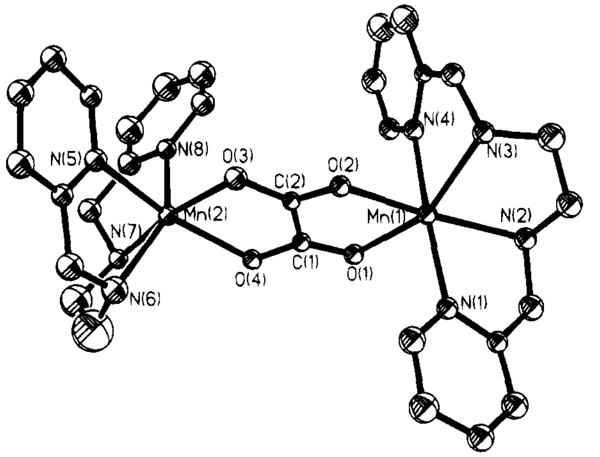

Figure 1. View of the [(bispicen)Mn(C_2O_4)Mn(bispicen)]$^{2+}$ cation in the crystals of the perchlorate salt (**1a**). The analogous Fe(II), Cu(II), and Zn(II) complexes are isomorphous with this Mn(II) complex. Hydrogen atoms in this and remaining structural figures are omitted for clarity. The complex exhibits the *cis*-α isomer at Mn(1) and the *cis*-*β* isomer at Mn(2).

(μ-Oxalato)bis(*N*,*N'*-bis(2-pyridylmethyl)-*N*,*N'*-bis(methyl)-1,2-ethanediamine)dicopper(II) Perchlorate, [(bispicMe$_2$en)Cu(C_2O_4)Cu(bispicMe$_2$en)](ClO_4)$_2$ (5c). The complex crystallizes in the centrosymmetric monoclinic space group $P2_1/n$ with two binuclear formula units in the cell. X-ray powder patterns indicate that the corresponding Co(II), Ni(II), and Zn(II) complexes [**3c**, **4c**, and **6c**, respectively] are isomorphous, and presumably isostructural, with this copper complex **5c**; the Mn(II) and Fe(II) analogues, **1c** (*vide supra*) and **2c**, are not isomorphous with these complexes or with each other, so that the six bispicMe$_2$en complexes fall into three isomorphous series. Data were collected in the range $4 < 2\theta < 50°$, the data gathered having $0 \le h \le +9$, $-26 \le k \le 0$, $-14 \le l \le +14$. The perchlorate anion is apparently disordered around a Cl−O bond [Cl−O(3)], so the remaining oxygen atoms are disordered into two sites with site occupancy factors set to 0.5. Hydrogen atoms were placed in fixed calculated positions (C−H = 0.96 Å); non-hydrogen atoms were refined anisotropically. The final values of the conventional *R* factors were $R = 0.0440$ and $R_w = 0.0499$ based on 1732 independent reflections with $I > 3\sigma(I)$. Positional parameters are listed in Table 7.

No single crystal structural analyses were conducted on the bispictn complexes (**1b**−**6b**), but X-ray powder patterns indicate that the Fe(II), Co(II), and Zn(II) complexes [**2b**, **3b**, and **6b**, respectively] are isomorphous with each other but not with the Mn(II) analogue, **1b**, or with the Ni(II) analogue **4b**; we did not isolate the copper(II) analogue, **5b** (*vide supra*).

Results and Discussion

Description of the Structures. [(Bispicen)Mn(C_2O_4)Mn(bispicen)](ClO_4)$_2$ (1a). The structure consists of binuclear [(bispicen)Mn(C_2O_4)Mn(bispicen)]$^{2+}$ cations and perchlorate anions. A view of the cation is shown in Figure 1. Principal bond distances are listed in Table 8.

Table 8. Selected Bond Lengths (Å) for $[(bispicen)Mn(C_2O_4)Mn(bispicen)]^{2+}$(**1A**)

Mn(1)−N(1)	2.213 (16)	Mn(1)−N(2)	2.278 (17)
Mn(1)−N(3)	2.281 (20)	Mn(1)−N(4)	2.259 (19)
Mn(1)−O(1)	2.175 (15)	Mn(1)−O(2)	2.184 (13)
Mn(2)−N(5)	2.234 (19)	Mn(2)−N(6)	2.274 (20)
Mn(2)−N(8)	2.254 (18)	Mn(2)−N(7)	2.251 (19)
Mn(2)−O(3)	2.149 (17)	Mn(2)−O(4)	2.198 (12)
Mn(1)−Mn(2)	5.626 (4)		

The binuclear cation consists of two $(bispicen)Mn^{II}$ units bridged by a bis-bidentate oxalate anion. As can be seen in Figure 1, the complex isolated is unusual in that one manganese center [Mn(1)] binds the ligand in the more common *cis*-α form in which the two pyridine rings of the ligand are *trans*, while that at the other manganese is *cis*-*β*. In recent years, we have examined the structures of numerous binuclear manganese complexes with bispicen and related ligands and have observed exclusively *cis*-α geometry at both metals.[15,17] In the chemistry of other metals, we occasionally observed *cis*-*β* geometry at both metals,[14,18] but the only previous example of mixed *cis*-α, *cis*-*β* geometry involves a di-μ-hydroxodichromium(III) complex of bispicen.[19]

The geometry at the two independent manganese(II) centers is roughly octahedral, with ligation provided by the four nitrogen atoms of the bispicen ligand and the oxygen atoms of the bridging oxalate. The geometry of the bridging Mn(1)−ox−Mn(2) unit is reminiscent of that in the copper(II) and nickel(II) structures alluded to earlier.[3−7] The Mn(1)···Mn(2) separation of 5.626 (4) Å in the present structure is slightly longer than those of 5.1−5.5 Å found in the dimeric copper(II) complexes.[3−6] The Mn−O bond lengths are in the range from 2.15 (2) to 2.20 (1) Å, and the Mn−N bonds are from 2.21 (2) to 2.28 (2) Å. Regrettably, the relative imprecision of the structure renders comparison of these metrical parameters with those of other structures less valuable.

To the precision available, the geometries of the perchlorate ions are comparable to those observed in recent determinations of the structure of this anion.[15,18,20]

$[(BispicMe_2en)Mn(C_2O_4)Mn(bispicMe_2en)](ClO_4)_2$ (1c). The structure consists of centrosymmetric binuclear $[(bispicMe_2en)Mn(C_2O_4)Mn(bispicMe_2en)]^{2+}$ cations and perchlorate anions. A view of the cation is shown in Figure 2. Principal bond distances are listed in Table 9.

As was the case in **1a** (with bispicen) and in all related species, the binuclear cation consists of two $(bispicMe_2en)Mn^{II}$ units bridged by a bis-bidentate oxalate anion. As can be seen in Figure 2, the complex isolated in **1c** exhibits the more common *cis*-α geometry at both metals; the same will be demonstrated for all other complexes studied here except **5c** (*vide infra*).

There is a crystallographic inversion center in the middle of the cation, bisecting the C(1)−C(1a) bond and relating the left side of the molecule in Figure 2 to the right side. Consequently, the geometries at the two manganese(II) centers are identical, with ligation provided by the four nitrogen atoms of the bispicMe₂en ligand and the oxygen atoms of the bridging oxalate as above. The geometry of the bridging Mn(1)−ox−Mn(1a) unit is again similar to that in the nickel(II) and copper(II) structures; $C_2O_4^{2-}$ ion is approximately planar (maximum deviation, 0.014 Å) and the two Mn atoms lie only 0.111 Å out of this plane. The C−O bond lengths of 1.249 (5) and 1.251 (5) Å in the oxalate ion are equal and normal for bidentate coordination. The C−C bond of 1.559 (8) Å is slightly longer than the values of 1.50−1.54 Å, usually observed in coordinated oxalate; the C−C bond length of 1.574 (2) Å in uncoordinated oxalate ion[21] is also very long, however, so the present observation is not surprising. The Mn(1)···Mn(1a) separation of 5.610 (1) Å in **1c** is comparable with that in **1a** above, and again longer than those of 5.1−5.5 Å found in the dimeric copper(II) complexes.[3−6] The Mn−O bond lengths of 2.160 (3) and 2.168 (3) Å [average 2.164 (6) Å] are apparently shorter than those in **1a**. The Mn−N bonds are unequal, the axial bonds (to pyridine) of 2.252 (4) and 2.256 (4) Å [average 2.254 (3) Å] being approximately 0.036 Å shorter than the equatorial distances of 2.286 (3) and 2.293 (3) Å [average 2.290 (5) Å]. Since this complex contains high-spin Mn(II), an isotropic d^5 ion, this observed lengthening of the equatorial bonds is attributable to the *trans* effect of the oxalate oxygen atoms.

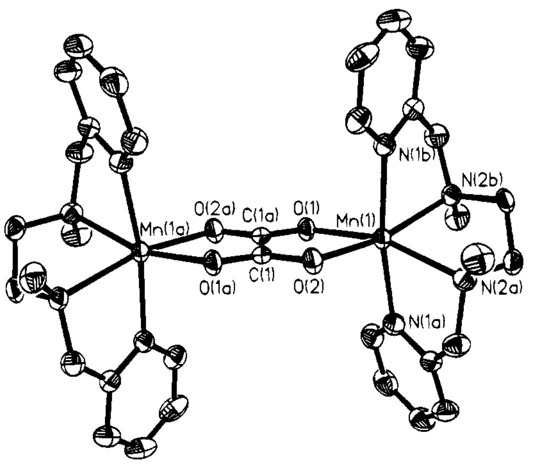

Figure 2. View of the $[(bispicMe_2en)Mn(C_2O_4)Mn(bispicMe_2en)]^{2+}$ cation in the crystals of the perchlorate salt (**1c**). In this and remaining structural figures, there is a crystallographic inversion center in the middle of the oxalate C−C bond, relating the left side of the molecule to the right side.

Table 9. Selected Bond Lengths (Å) for $[(bispicMe_2en)Mn(C_2O_4)Mn(bispicMe_2en)]^{2+}$(**1c**)

Mn(1)−O(1)	2.168 (3)	Mn(1)−O(2)	2.160 (3)
Mn(1)−N(1A)	2.256 (4)	Mn(1)−N(2A)	2.293 (3)
Mn(1)−N(1B)	2.252 (4)	Mn(1)−N(2B)	2.286 (3)
Mn(1)−Mn(1A)	5.610 (1)		

The perchlorate ions in the structure are ordered, with Cl−O bond lengths in the range 1.387 (5)−1.462 (5) Å [average, 1.42 (3) Å] and O−Cl−O bond angles of 106.1−114.9 (3)° [average, 109 (3)°]; these metrical parameters are again comparable to those observed in recent determinations of the structure of this anion.[15,18,20]

$[(Bispicen)Co(C_2O_4)Co(bispicen)](ClO_4)_2{\cdot}H_2O$ (3a). The structure consists of centrosymmetric binuclear $[(bispicen)Co(C_2O_4)Co(bispicen)]^{2+}$ cations which are hydrogen bonded to solvent water molecules and perchlorate anions. A view of the cation is shown in Figure 3. Principal bond distances are listed in Table 10.

---

(17) (a) Collins, M. A.; Hodgson, D. J.; Michelsen, K.; Towle, D. K. *J. Chem. Soc., Chem. Commun.* **1987**, 1659−1660. (b) Goodson, P. A.; Glerup, J.; Hodgson, D. J.; Michelsen, K.; Pedersen, E. *Inorg. Chem.* **1990**, *29*, 503−508. (c) Goodson, P. A.; Glerup, J.; Hodgson, D. J.; Michelsen, K.; Weihe, H. *Inorg. Chem.* **1991**, *30*, 4909−4914.

(18) Arulsamy, N.; Goodson, P. A.; Hodgson, D. J.; Glerup, J.; Michelsen, K. *Inorg. Chim. Acta* **1994**, *216*, 21−29.

(19) Heinrichs, M. A.; Hodgson, D. J.; Michelsen, K.; Pedersen, E. *Inorg. Chem.* **1984**, *23*, 3174−3180.

(20) See, for example: Glerup, J.; Goodson, P. A.; Hodgson, D. J.; Michelsen, K.; Nielsen, K. M.; Weihe, H. *Inorg. Chem.* **1992**, *31*, 4611−4616.

(21) Hodgson, D. J.; Ibers, J. A. *Acta Crystallogr., Sect. B* **1969**, *25*, 469−477.

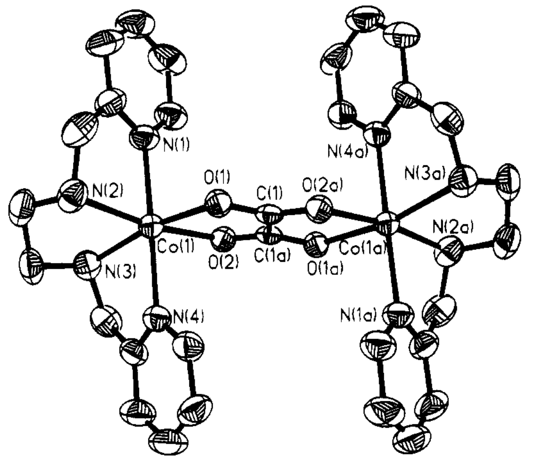

Figure 3. View of the [(bispicen)Co(C_2O_4)Co(bispicen)]$^{2+}$ cation in the crystals of the perchlorate salt (**3a**). The analogous Ni^{II} complex is isomorphous with this Co^{II} complex.

Table 10. Selected Bond Lengths (Å) for [(bispicen)Co(C_2O_4)Co(bispicen)]$^{2+}$(**3a**)

Co(1)–N(1)	2.132 (5)	Co(1)–N(2)	2.145 (4)
Co(1)–N(3)	2.144 (4)	Co(1)–N(4)	2.150 (5)
Co(1)–O(1)	2.093 (3)	Co(1)–O(2)	2.096 (3)
Co(1)–Co(1A)	5.432 (2)		

The cation is fundamentally similar to that of the Mn complex cation in **1c**, above. Thus, the complex is in the *cis*-α geometry at both metals. There is a crystallographic inversion center in the middle of the cation, bisecting the C(1)–C(1a) bond. The geometry of the bridging Co(1)–ox–Co(1a) unit is normal; $C_2O_4^{2-}$ ion is planar (maximum deviation, 0.001 Å), and the two Co atoms lie 0.193 Å out of this plane. The C–O bond lengths of 1.242 (6) and 1.259 (5) Å [average, 1.251 (12) Å] in the oxalate ion are normal for bidentate coordination. The C–C bond of 1.551 (9) Å is again long. The Co–O bond lengths of 2.093 (3) and 2.096 (3) Å [average 2.094 (2) Å] are approximately 0.07 Å shorter than the Mn–O bonds in **1c**, consistent with the smaller radius of Co(II). The Co(1)···Co(1a) separation is 5.432 (2) Å, again shorter than the corresponding separation in the manganese complexes. The Co–N bonds of 2.132–2.150 Å [average 2.143 (8) Å] are approximately equal.

The solvent water molecule apparently forms a hydrogen bond to the coordinated oxalate anion, the O(1w)···O(1) separation of 2.920 Å being suggestive of a moderately strong hydrogen bond,[22] but in the absence of the location of the water protons any further analysis would be speculative.

The perchlorate anions are again ordered, with geometries consistent with those in other structures.

[(Bispicen)Cu(C_2O_4)Cu(bispicen)](ClO_4)$_2$ (5a). The structure consists of binuclear [(bispicen)Cu(C_2O_4)Cu(bispicen)]$^{2+}$ cations and perchlorate anions. A view of the cation is shown in Figure 4, and principal bond distances are listed in Table 11.

Like the isomorphous Mn(II) complex **1a**, the isomer isolated here is the uncommon *cis*-α , *cis*-β isomer. The oxalate group is not planar, with deviations of up to 0.12 Å from the least-squares plane.

The cation is, of course, fundamentally similar to that in the Mn(II) complex **1a**, but the d^9 electronic configuration gives rise to an important geometrical distinction. At the α site, Cu(1), the axial bonds to the pyridine nitrogen atoms are short, while the other bonds are long, giving rise to an axially compressed structure as in the bispicMe$_2$en structure *vide infra*. At the β site, Cu(2), the structure is axially elongated, but the long axis involves the Cu–O(3) and Cu–N(8) bonds.

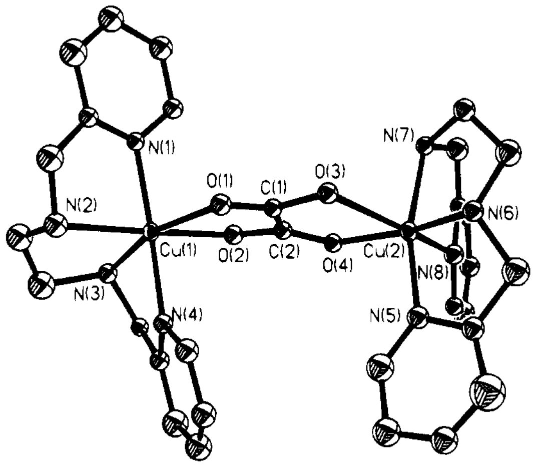

Figure 4. View of the [(bispicen)Cu(C_2O_4)Cu(bispicen)]$^{2+}$ cation in the crystals of the perchlorate salt (**5a**). The complex is isomorphous with the analogous manganese (see Figure 1), iron, and zinc complexes.

Table 11. Selected Bond Lengths (Å) for [(bispicen)Cu(C_2O_4)Cu(bispicen)]$^{2+}$(**5a**)

Cu(1)–O(1)	2.169 (17)	Cu(1)–O(2)	2.223 (14)
Cu(1)–N(1)	2.018 (16)	Cu(1)–N(2)	2.159 (20)
Cu(1)–N(3)	2.203 (21)	Cu(1)–N(4)	2.020 (18)
Cu(2)–O(3)	2.366 (13)	Cu(2)–O(4)	2.001 (17)
Cu(2)–N(5)	1.978 (19)	Cu(2)–N(6)	1.945 (20)
Cu(2)–N(7)	2.049 (16)	Cu(2)–N(8)	2.206 (21)
Cu(1)–Cu(2)	5.608		

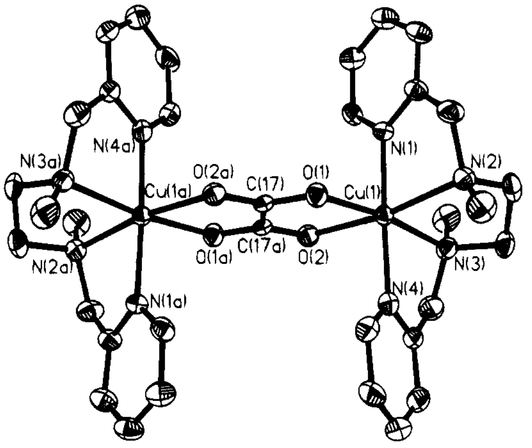

Figure 5. View of the [(bispicMe$_2$en)Cu(C_2O_4)Cu(bispicMe$_2$en)]$^{2+}$ cation in the crystals of the perchlorate salt (**5c**). The analogous Co^{II}, Ni^{II}, and Zn^{II} complexes are isomorphous with this Cu^{II} complex.

Table 12. Selected Bond Lengths (Å) for [(bispicMe$_2$en)Cu(C_2O_4)Cu(bispicMe$_2$en)]$^{2+}$(**5c**)

Cu(1)–O(1)	2.060 (5)	Cu(1)–O(2)	2.183 (5)
Cu(1)–N(1)	2.041 (5)	Cu(1)–N(2)	2.197 (6)
Cu(1)–N(3)	2.127 (6)	Cu(1)–N(4)	2.046 (5)
Cu(1)–Cu(1A)	5.494 (2)		

[(BispicMe$_2$en)Cu(C_2O_4)Cu(bispicMe$_2$en)](ClO_4)$_2$ (5c). The structure consists of centrosymmetric binuclear [(bispicMe$_2$en)-Cu(C_2O_4)Cu(bispicMe$_2$en)]$^{2+}$ cations which are well separated from perchlorate anions. A view of the cation is shown in Figure 5. Principal bond distances are listed in Table 12.

The cation is fundamentally similar to those of the Mn and Co cations in **1c** and **3a**, above. Thus, the geometry at the copper centers is *cis*-α, and there is a crystallographic inversion center in the middle of the cation, bisecting the C(17)–C(17a)

---

(22) Hamilton, W. C.; Ibers, J. A. *Hydrogen Bonding in Solids*; Benjamin: New York, 1968.

bond. It is, perhaps, noteworthy in this regard that most of the other binuclear μ-oxalatodicopper(II) complexes whose structures have been reported[3-6] have exhibited five-coordinate geometries rather than the *pseudo*-octahedral six-coordinate structure observed here. $C_2O_4^{2-}$ ion is approximately planar, and the two Cu atoms lie approximately in this plane. The C—O bond lengths of 1.227 (8) and 1.262 (9) Å are apparently unequal in this case, however, and the smaller of these values [C(17)—O(2a)] is the shortest that we have found in the literature for related species.[3-6] The C—C bond of 1.571 (14) Å is comparable to that in uncoordinated oxalate ion.[21] The Cu(1)···Cu(1a) separation is 5.494 (2) Å. The Cu—O bond lengths of 2.060 (5) and 2.183 (5) Å are also unequal.

The Cu—N bonds are unequal, the axial bonds (to pyridine) of 2.041 (5) and 2.046 (5) Å [average 2.044 (4) Å] being approximately 0.12 Å shorter than the equatorial distances of 2.127 (6) and 2.197 (6) Å [average 2.162 (49) Å]. Since this complex contains the d^9 ion, this observed shortening of the axial bonds is attributable to a Jahn—Teller distortion of the complex, giving rise in the present case to an axially-compressed (2 + 4) geometry rather than the more common axially-elongated (4 + 2) structure. (The magnetic significance of this structural feature will be discussed in a subsequent section (*vide infra*).)

The perchlorate anions are disordered. They were approximately, although not entirely satisfactorily, fitted to a model in which two equally occupied sets of oxygen atom positions share a common Cl—O bond [Cl—O(3)], giving rise to two approximate tetrahedra which are rotated by approximately 60° from each other; this kind of disorder has been observed in several earlier determinations of the structure of this ion.[18,23]

NMR Spectra. The solid state ^{13}C NMR spectra of the zinc complexes **6a—c** are very revealing. The aliphatic (low-field) region is surprisingly insensitive to coordination, and the spectra of the zinc(II) complexes are not significantly different from those of the protonated ligands, $(AH)_4^{4+}$. This result is unexpected, since on the basis of the sensitivity of this region in the spectra of complexes of bis(2-pyridylmethyl)amine,[20] we had anticipated that the existence of both α- and β-isomers in **6a** would lead to a more complex spectrum.

The aromatic region of the spectra, shown in Figure 6, is more rewarding. Although the spectrum of the uncomplexed protonated bispicen ligand is, of course, much simpler than that of protonated bispicMe$_2$en, the spectrum of the bispicen complex **6a** in the region 120 —170 ppm is clearly much more complex than that of the bispicMe$_2$en complex **6c**. It is particularly noteworthy that oxalato carbon atoms at 167.8 ppm are unsplit in the spectrum of **6c** but are split into two peaks at 167.9 and 168.4 ppm in that of **6a**; this splitting is attributable to the presence of two isomers in **6a**.

The above comparison allows some informed discussion concerning the structure of **6b** and, consequently, of the isomorphous Fe(II) and Co(II) complexes of bispictn, **2b** and **3b**. The oxalato carbon peak at 169.2 ppm is unsplit, suggesting the presence of only a single isomer. However, the aromatic portion of the spectrum is evidently more complex than that of **6c** while less complex than that of **6a**. These observations are consistent with the conclusion that the complex in **6b** contains the *cis-β*, *cis-β* geometry; in the β-isomer, one aromatic ring is axial while the other is equatorial, leading to a more complex spectrum than in the α,α-isomer in **6c**.

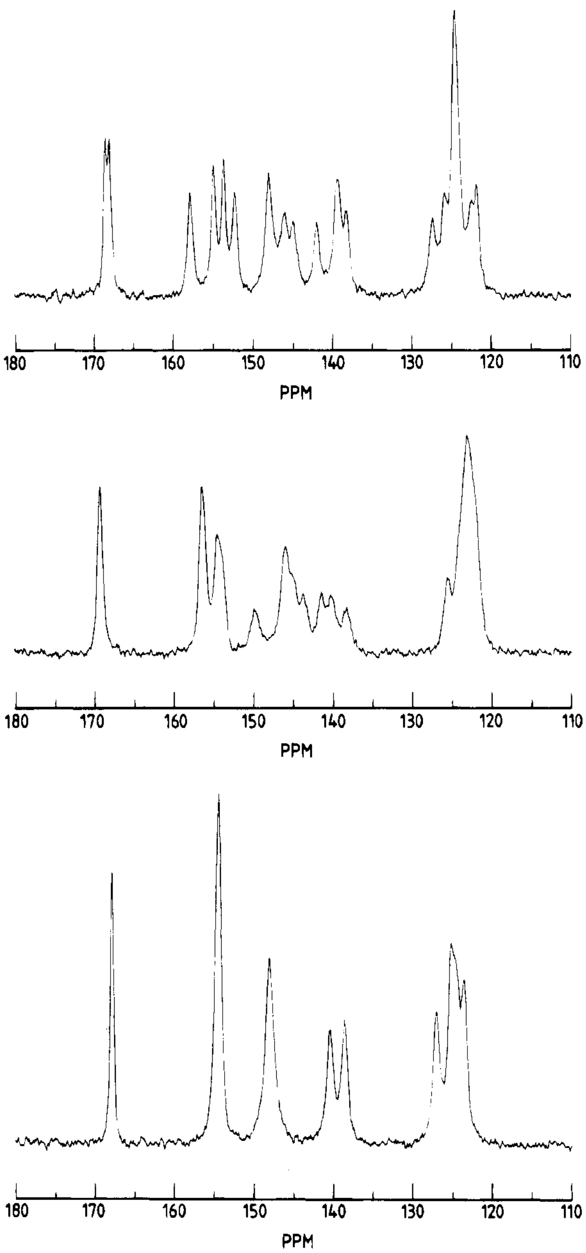

Figure 6. Solid state ^{13}C NMR spectra (aromatic region) of the zinc(II) complexes of bispicen (**6a**) (top); bipictn (**6b**) (middle); and bispicMe$_2$en (**6c**) (bottom).

There is some structural precedent for such a conclusion. The presence of the additional methylene group in bispictn gives rise to a six-membered chelate ring in the complexes, and the *cis-β* geometry has been observed in several complexes of this ligand[14,18,24,25] but only rarely in complexes of related ligands containing only five-membered rings.[19] Thus, while in the absence of crystallographic evidence a definitive structural assignment is precluded, the present interpretation of the NMR spectra is internally consistent and leads to a conclusion that is not entirely unexpected.

Magnetic Properties. The magnetic properties of the present series of complexes are of considerable interest. As we noted above, the present complexes of manganese (**1a—c**), iron (**2a—c**), and cobalt (**3a—c**) represent the first examples of simple

---

(23) (a) Hodgson, D. J.; Zietlow, M. H.; Pederen, E.; Toftlund, H. *Inorg. Chim. Acta* **1988**, *149*, 111—117. (b) Oki, A. R.; Glerup, J.; Hodgson, D. J.; *Inorg. Chem.* **1990**, *29*, 2435—2441.

(24) Glerup, J.; Hazell, A.; Michelsen, K. *Acta Chem. Scand.* **1991**, *45*, 1025—1031.

(25) Hodgson, D. J.; Michelsen, K.; Pedersen, E.; Towle, D. K. *J. Chem. Soc., Chem. Commun.* **1988**, 426—428; *Inorg. Chem.* **1991**, *30*, 815—822.

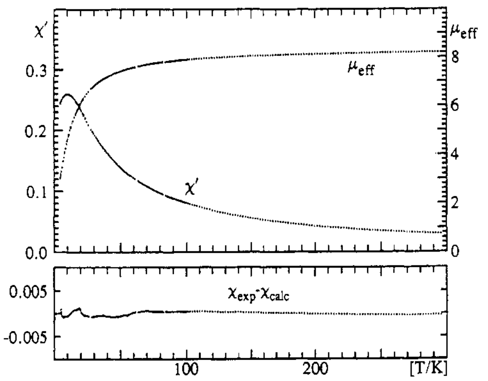

Figure 7. (Top) Magnetic susceptibility (cgs units) and the magnetic moment of $[(\text{bispictn Mn})_2\text{ox}](\text{ClO}_4)_2\cdot 0.5\text{H}_2\text{O}$. (Bottom) The difference between the measured and calculated susceptibility.

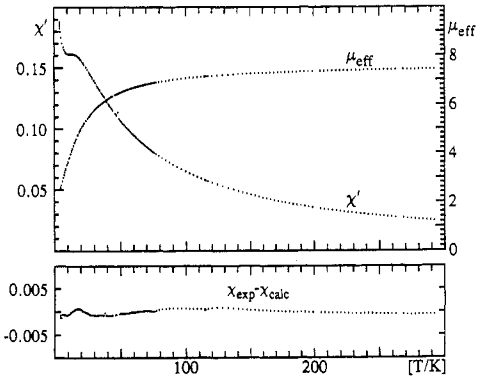

Figure 8. (Top) Magnetic susceptibility (cgs units) and the magnetic moment of $[(\text{bispicen Fe})_2\text{ox}](\text{ClO}_4)_2$. (Bottom) the difference between the measured and calculated susceptibility.

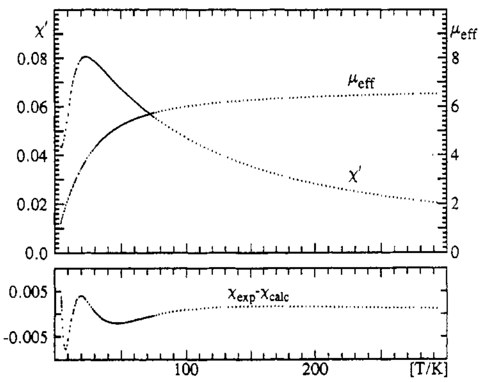

Figure 9. (Top) Magnetic susceptibility (cgs units) and the magnetic moment of $[(\text{bisMe}_2\text{picen Co})_2\text{ox}](\text{ClO}_4)_2\cdot\text{H}_2\text{O}$. (Bottom) the difference between the measured and calculated susceptibility.

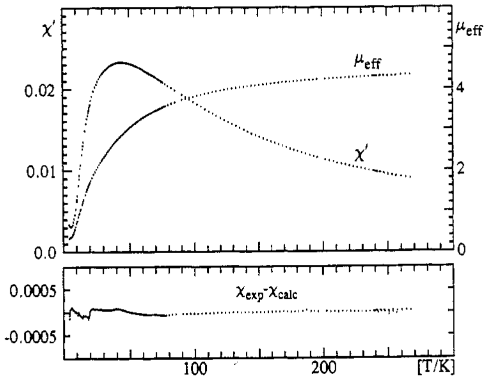

Figure 10. (Top) Magnetic susceptibility (cgs units) and the magnetic moment of $[(\text{bispicen Ni})_2\text{ox}](\text{ClO}_4)_2\cdot 3\text{H}_2\text{O}$. (Bottom) the difference between the measured and calculated susceptibility.

binuclear μ-oxalato complexes of these metals, and necessarily there are no related complexes to whose magnetic properties these systems may be compared. Fortunately, there are several known complexes of nickel(II) and copper(II) which have been thoroughly examined.[3-7]

For the manganese complexes, the effective magnetic moment at room temperature is 8.3−8.4 μ_B, in good agreement with the spin-only value of 8.37 μ_B expected for two noninteracting high-spin d^5 Mn^{II} ions. As is shown for the case of the bispictn complex (**1b**) in Figure 7, the effective magnetic moment declines slowly with decreasing temperature until approximately 40 K, when it begins to decline more rapidly, reaching a value of approximately 3 μ_B at 5 K. The magnetic susceptibility for the complex exhibits a maximum at 10.4 K.

The behavior of the iron complexes is similar to that observed for the manganese complexes and is shown for the bispicen complex (**2a**) in Figure 8. The effective magnetic moment at room temperature is 7.4 μ_B, close to the spin-only value of 6.93 μ_B expected for two noninteracting high-spin d^6 Fe^{II} ions. The magnetic susceptibility for the complex exhibits a maximum at 13.2 K. The susceptibility increases on further cooling, which is consistent with the presence of some small quantity of monomeric impurity in the sample.

The properties of the cobalt complexes are again similar to those above. The effective magnetic moments at room temperature are 6.7−7.2 μ_B, significantly larger than the spin-only value of 5.48 μ_B expected for two noninteracting high-spin d^7 Co^{II} ions. As is shown for the case of the bispicMe2en complex (**3c**) in Figure 9, the magnetic susceptibility for the complex exhibits a maximum at 23.2 K.

For the nickel(II) complexes, the room temperature effective magnetic moments are in the range 4.2−4.4 μ_B, close to the expected value of 4.0 μ_B for two noninteracting d^8 Ni^{II} ions. As is shown for the case of the bispicen complex (**4a**) in Figure 10, the magnetic susceptibility for the complex exhibits a maximum at 43.7 K.

The copper(II) complexes exhibit room temperature magnetic moments of 2.8 μ_B, close to the expected value of 2.45 μ_B for two noninteracting d^9 Cu^{II} ions. The moments decline very slightly over the entire temperature range, and the magnetic susceptibilities of the complexes do not exhibit a maximum above 4 K.

Previously we have used isotropic operators to describe the magnetic interactions in dinuclear complexes. However, for this series of complexes the ground states of the individual metal ions, except for the Mn^{II} ion, are expected to be very anisotropic. The magnetic susceptibility of an anisotropic powdered compound was approximated by the average of the susceptibilities in the x, y, and z directions.

The temperature dependence of the average magnetic susceptibilities $\chi'_{\text{mol.exp}}$ were approximated by eq 1 by minimization

$$\chi'_{\text{mol.exp}} \approx \chi'_{\text{mol.calc}} = \frac{1}{3}\sum_{j=x,y,z} \frac{-N}{B}\,\frac{\sum_i (\partial E_{ij}/\partial B)\exp(-E_{ij}/kT)}{\sum_i \exp(-E_{ij}/kT)} + K + C/T \qquad (1)$$

of eq 2 within the framework of nonlinear regression analysis.

$$\sum_T \frac{[\chi'_{\text{mol.exp}}(T) - \chi'_{\text{mol.calc}}(T)]^2}{\sigma^2(\chi') + (\partial\chi/\partial T)^2\sigma^2(T)} \qquad (2)$$

Table 13. Magnetic Parameters For the Complexes

metal	ligand	$g_x = g_y$	g_z	J/cm^{-1}	D/cm^{-1}	monomeric impurity %
Mn^{II}	bispicen	2.02		1.91	0.24	2
	bispictn	2.01		2.48	0.07	1.4
	bisMe$_2$picen	1.99		2.04	0.07	0.7
Fe^{II}	bispicen	2.5	2.0	5.1	2.8	5
	bispictn	2.2	1.6	6.1	4.9	5
	bisMe$_2$picen	2.6	1.6	6.6	1.4	6
Co^{II}	bispicen	2.0	3.0	8.8	3.2	~0
	bispictn	2.4	2.1	9.4	5.2	2
	bisMe$_2$picen	2.5	2.4	11.4	7.0	0.4
Ni^{II}	bispicen	2.25		32.03	2.6	1.4
	bispictn	2.11		34.48	1.4	1.4
	bisMe$_2$picen	2.10		33.71	1.6	1.2
Cu^{II}	bispicen	2.28		2.3		
	bispictn					
	bisMe$_2$picen	2.24		2.14		

$\sigma(\chi')$ and $\sigma(T)$ are the estimated standard deviations on the measured magnetic susceptibility and temperature, respectively. In eq 1, C/T accounts for paramagnetic impurities and K accounts for temperature independent paramagnetism and minor deviations in the correction for diamagnetism. The energies E_i of the ground state manifolds for the dinuclear complexes were obtained by means of the anisotropic spin Hamilton operator eq 3, where we have assumed that the g-values and the D-values

$$\hat{H} = \sum_{i=a,b}\sum_{j=x,y,z} g_{ij}\mu_B \hat{S}_i{\cdot}\hat{H} + \sum_{i=a,b} D_i\left[\hat{S}_{iz}^2 - \frac{1}{3}S_i(S_i+1)\right] + J\hat{S}_a{\cdot}\hat{S}_b \quad (3)$$

for the two metal ions are identical; this may be an imperfect assumption for the complexes **1a**, **2a**, and **5a**, which exhibit the unsymmetrical *cis*-α, cis-β geometry.

The results of the fitting are shown in Table 13. For the Mn^{II}, Ni^{II}, and Cu^{II} complexes we have forced the g-values to be isotropic. From Table 13 and from Figure 8 one sees that the fitting for Fe^{II} gives 5% monomeric impurities and a bad agreement at low temperature. We think this is merely becauce of an imperfect model. For the Cu^{II} complexes, which have a small interaction, the constant C in eq 1 has to be kept constant, otherwise the fitting is unstable. We are perfectly aware of the questionable value of fitting the magnetic data for the Fe^{II} and Co^{II} complexes to eq 3. The g-values and the D-values vary in an unpredictable manner, while the variation of the J-values is more smooth, however, we believe tentatively that the J-values are representative of the magnetic interactions in these complexes.

Kahn and co-workers[3] have demonstrated that for the copper(II) complexes the magnetic exchange pathway is dominated by the interactions between the metal $x^2{-}y^2$ orbitals and the oxalate σ orbitals. For all of the Mn, Fe, Co, and Ni complexes, in any geometry, the metal $x^2{-}y^2$ orbital is half-occupied and is aligned to allow overlap with the oxalate σ orbitals. For the present Ni complexes, the observed J-values of 32.03−34.48 cm^{-1} are very similar to those of 34−39 cm^{-1} reported for other symmetric Ni(II) complexes.[7a,f,h] While we do not have any single crystal structures for our nickel complexes, we do know that **4a** is isomorphous with **3a** and that **4c** is isomporphous with **5c**, so both of these complexes are known to be centrosymmetric dimers. This is of significance because other workers have shown that unsymmetrical dimers generally exhibit lower J-values of approximately 26 cm^{-1}.[7g]

For these series of complexes we would also expect the σ interactions described above would dominate the magnetic interactions. On the other hand, π interactions could also be of importance, however, we can exclude this possibility. The t$_2$ orbitals of Mn^{II} are half-filled, allowing maximal antiferromagnetic π interactions, while those in Ni^{II} are filled, allowing no antiferromagnetic π interactions. Hence, the precence of significant π contribution to the magnetic exchange would cause an opposite trend to that observed in Table 13. Consequently, we may deduce that the σ interaction is the dominent magnetic pathway for the entire series Mn^{II}, Fe^{II}, Co^{II}, and Ni^{II}.

Because of the lack of similar complexes, we are forced to make a comparison of the antiferromagnetic interactions between the different metal atoms. However, we cannot just compare the experimental J-values.[26] We have previously published a model[27] for the antiferromagnetic interaction which enables us to compare the magnetic interactions in these complexes. In this model, the antiferromagnetic interaction emerge as a result of configuration interaction between the ground levels and charge transfer levels where an electron is moved from one metal to the other metal and *vice versa*. A recent *ab initio* calculation[28] has confirmed this model for the antiferromagnetic interaction.

From the experiments we concluded that the main interaction in the complexes from manganese to nickel was between the half-filled $x^2{-}y^2$ orbitals on the two metal atoms. In the following we will only consider the interaction between these orbitals. The nondiagonal elements were calculated between the functions for the lowest levels and the charge transfer levels, as previously described.[27] The J-values, the triplet−singlet separations, are calculated as the square of the nondiagonal elements divided by the energy of the charge transfer states and are given in eq 4.

$$\begin{aligned}
J_{\mathrm{Cu}} &= 4[\langle (x^2-y^2)_{\mathrm{a}}|V_{\mathrm{ab}}|(x^2-y^2)_{\mathrm{b}}\rangle]^2/E_{\mathrm{CT}}\\
J_{\mathrm{Ni}} &= [\langle (x^2-y^2)_{\mathrm{a}}|V_{\mathrm{ab}}|(x^2-y^2)_{\mathrm{b}}\rangle]^2/E_{\mathrm{CT}}\\
J_{\mathrm{Co}} &= {}^4/_9[\langle (x^2-y^2)_{\mathrm{a}}|V_{\mathrm{ab}}|(x^2-y^2)_{\mathrm{b}}\rangle]^2/E_{\mathrm{CT}}\\
J_{\mathrm{Fe}} &= {}^1/_4[\langle (x^2-y^2)_{\mathrm{a}}|V_{\mathrm{ab}}|(x^2-y^2)_{\mathrm{b}}\rangle]^2/E_{\mathrm{CT}}\\
J_{\mathrm{Mn}} &= {}^4/_{25}[\langle (x^2-y^2)_{\mathrm{a}}|v_{\mathrm{ab}}|(x^2-y^2)_{\mathrm{b}}\rangle]^2/E_{\mathrm{CT}} \qquad (4)
\end{aligned}$$

The different factors in front of the theoretical J-values are caused by the fact that for the Cu^{II} case there is only one magnetic orbital on each metal atom. For the Ni^{II} case there are two magnetic orbitals on each metal atom, for the Fe^{II} case there are three magnetic orbitals on each atom, for Co^{II} case there are four on each atom, and for the Mn^{II} case there are five magnetic orbitals on each atom; however, in each case we are only considering the interaction between one set of magnetic orbitals, *i.e.*, the $x^2 - y^2$ orbitals. From this we can deduce that the relative size of the factors are equal to $1/n^2$, where n is the number of unpaired electrons. One could say that the exchange interaction is "diluted" by the unpaired electrons which do not participate.

In Figure 11 is shown a plot of the calculated J-values as a function of the experimental J-values. The points are almost on a straight line, which means there is an excellent correlation between the calculated and measured J-values. In this correlation we have assumed that the energy of the charge transfer states E_{CT} are almost the same for the different metal atoms. From the above correlation we can conclude that the magnetic

---

(26) Glerup, J.; Goodson, P. A.; Hodgson, D. J.; Weihe, H. *Inorg. Chim. Acta* **1993**, *212*, 281−288.

(27) Glerup, J. *Acta Chem. Scand.* **1972**, *26*, 3775−3785.

(28) Fink, K.; Fink, R.; Staemmler, V. *Inorg. Chem.* **1994**, *33*, 6219−6229.

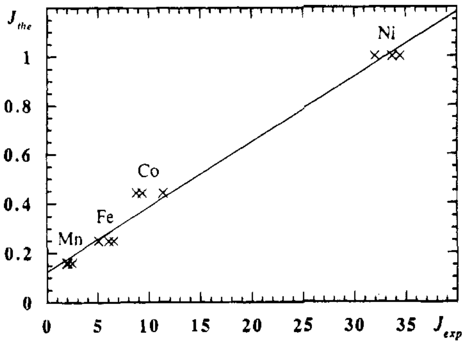

Figure 11. Theoretical J-values from eq 4 plotted against the experimental J-values taken from Table 13.

interaction between the $x^2 - y^2$ orbitals on two metal atoms have almost the same size among the metals Mn^{II}, Fe^{II}, Co^{II}, and Ni^{II}. For the Cu^{II} complexes which do not follow the above correlation we must conclude that the unpaired electrons are not in $x^2 - y^2$ orbitals but rather in the z^2 orbitals (vide infra).

The very small antiferromagnetic interactions in the copper(II) complexes here are unexpected. Kahn and his co-workers have demonstrated that five-coordinate μ-oxalatodicopper(II) complexes can be designed with J-values from approximately zero to approximately 400 cm^{-1} by modifying the ligands. The actual role of this ligand modification is to realign the metal magnetic orbital relative to the oxalate σ orbital. The concept is that if we have two square planar Cu(II) centers, leading to an entirely planar [LC(μ-ox)CuL] array, the $x^2 - y^2$ Cu magnetic orbital will be ideally directed toward the oxalate σ orbitals, and the antiferromagnetic interaction will be maximized. Consequently, complexes with this square planar or (4 + 1) tetragonal pyramidal geometry at both copper centers give rise to J-values near 400 cm^{-1}.[3,6a–c] Presumably, axially elongated (4 + 2) *pseudo*-octahedral geometry would also tend to maximize the interaction. If the symmetry of the dimer is reduced by virtue of the presence of different coordinating ligands at the two metal centers, there is a decrease in the magnitude of J because there is now an energy gap between the two magnetic orbitals.[6c,d,29]

If the geometry at one of the copper centers is so that its magnetic orbital does not overlap with the oxalate σ orbital, we will observe intermediate coupling with J-values of approximately 75 cm^{-1}.[3] In Kahn's case, this was achieved by designing a system in which one of the oxalate oxygen atoms is in the base plane of a tetragonal pyramid while the other is apical, thereby locating the magnetic orbital on that copper center perpendicular to the oxalate σ orbital. Finally, if the geometry at both copper centers is so that neither magnetic orbital overlaps with the oxalate σ system, we have very weak coupling [J of approximately 14 cm^{-1}].[3]

Our ligands force six-coordinate geometry at the Cu^{II} metal, and this result is a very weak magnetic interaction. The reason for this can be deduced from the details of the observed structures. If we examine the structure of the bispicen complex **5a** in Figure 4, we see that at the *cis*-α site Cu(1) we have the relatively uncommon axially-compressed (2 + 4) geometry, with the short axis defined by the Cu−N(1) and Cu−N(4) bonds of 2.018 (16) and 2.020 (18) Å which is perpendicular to the oxalate plane. Consequently, in the axial system we have defined, this center has a z^2 magnetic orbital which overlaps very poorly with the oxalate σ orbital; the situation is orbitally analogous to that of a trigonal bipyramidal center.[3] At the *cis*-β site Cu(2), we have the common (4 + 2) axially elongated system, but the long axis is defined by the Cu−O(3) and Cu−N(8) bonds which are 0.36 and 0.22 Å longer than the average values of the other Cu(2)−O and Cu(2)−N bond lengths, respectively. Hence, we have described a system analogous to the tetragonal pyramid obtained by Kahn (*vide supra*) in which one oxalate oxygen atom is in the basal plane while the other is axial, and once again the magnetic orbital is in a plane perpendicular to the oxalate σ orbital. Hence, the structure reveals that in complex **5a** both magnetic orbitals have a poor overlap with oxalate σ orbital.

Examination of the structure of complex **5c** (Figure 5) reveals an apparent lengthening of the Cu−O(2), Cu−N(2) axis in a (4 + 2) structure, again leading to the situation in which one oxalate oxygen atom is in the basal plane while the other is axial, and once again the magnetic orbital is in a plane perpendicular to the oxalate σ orbital.

It should also be noted that the present Cu^{II} complexes have J-values close to zero, while the five-coordinate complexes previously reported[3,4b] show J-values in the range 15−20 cm^{-1}. Evidently, the present distorted six-coordinate geometries permit significantly weaker antiferromagnetic interactions than have previously been reported for μ-oxalatodicopper(II) complexes.

EPR Spectra. Low-temperature solid state spectra of these compounds were not sufficiently magnetically diluted, giving rise to uncharacteristic spectra which could not be identified as genuine dinuclear spectra. Attempts to dilute the compounds in the Zn^{II} complexes resulted in monomeric spectra, as did frozen solution glass spectra in N-methylformamide.

Acknowledgment. This work was supported by the National Science Foundation through Grant No. CHE-9007607 (to D.J.H.) and by the Scientific Affairs Division, North Atlantic Treaty Organization (NATO), through Grant No. CRG 910277 (to J.G., D.J.H., and K.M.).

Supporting Information Available: Tables of complete coordinates, bond lengths, bond angles, anisotropic displacement parameters, and hydrogen atom coordinates for each of the complexes **1a, 1c, 3a, 5a,** and **5c** (33 pages). For ordering information, see any current masthead page. Listings of observed and calculated structure amplitudes for all five complexes are available from D.J.H.

IC9503444

---

[29] Chauvel, C.; Girerd, J. J.; Jeannin, Y.; Kahn, O.; Lavigne, G. *Inorg. Chem.* **1979**, *18*, 3015−3020.